How to cite: *Angew. Chem. Int. Ed.* **2026**, e23011
doi.org/10.1002/anie.202523011

Photochemistry

Dibenzazepine Bridged Network Polymeric Phthalocyanines as Degradable Heterogeneous Photocatalysts

Erem Ahmetali, Azra Kocaarslan, Vanessa Trouillet, Stefan Heißler, and Stefan Bräse**

This paper is dedicated to the late Prof. Dr. Yusuf Yagci, who was an exceptionally inspiring and supportive mentor to many young researchers

Abstract: Recyclability and energy efficiency are inevitable requirements in today´s synthetic materials, as well as functional efficiency. Network polymeric phthalocyanines (NP-Pcs) are versatile molecular frameworks which widely utilized in energy and electron transfer demanding applications, but light hasn´t played a role before in their "design and degradation". Herein, we introduce photodynamic dibenzazepine moiety into NP-Pcs to obtain degradable heterogeneous photocatalysts (NP-ZnPc and NP-CoPc). Singlet oxygen generation efficiency of NP-ZnPc is found to be high, almost completely quenching the absorbance of diphenylisobenzofuran (DPBF) within 30 s upon red light ($\lambda = 630$ nm) irradiation. Supplementary reactions show that NP-ZnPc has the capability to oxidize methylphenyl sulfide with 100% yield in 4 h reaction time. Subsequently, PET-RAFT polymerization of 2-hydroxyethyl methacrylate is successfully initiated by NP-ZnPc in the presence of a chain transfer agent upon red light ($\lambda = 647$ nm) irradiation. The linearity in the increase in molecular weight (14,400–21,200 g/mol) and the decrease in monomer concentration ($\ln([M]_0/[M]_t = 0.6–3.4$) demonstrate the living characteristic of PET-RAFT polymerization. Thanks to its heterogeneous nature, NP-ZnPc is readily recovered and reused after polymerization up to three consecutive cycles without significant loss of performance. Notably, complete degradation of NP-Pcs was achieved under 254 nm light irradiation.

Introduction

Recycling is a fundamental strategy for resource conservation, waste reduction, and environmental sustainability, contributing to a circular economy by extending the lifecycle of materials.[1,2] Recycling of traditional polymers is challenging because their covalent bonds are irreversible and require energy-intensive processes.[3] However, it is not only crucial for traditional polymers but also for any synthesized material to ensure sustainable resource utilization, cost-effectiveness, and minimal environmental impact.[4] Dynamic covalent bonds (DCBs) are reversible covalent bonds that can break and reform under certain conditions, and they provide a revolutionary solution to recyclability, offering enhanced material durability, repairability, and re-processability.[5–8] Photo dynamic covalent bonds (PDCBs), which are a subclass of DCBs, utilize the light energy to trigger reversible bond formation under mild conditions, significantly reducing energy consumption in material processing.[9,10] The regulation of chemical bonds through light exposure provides a high degree of versatility in modulating specific material properties in addition to precise spatial and temporal control.[11,12] Stilbene, coumarin and anthracene are significant representatives of PDCB and have the ability to give [2 + 2] and [4 + 4] cycloaddition reactions under certain light irradiation.[13] The photocycloaddition reactions proceed by excitation of the

[*] Dr. E. Ahmetali, Prof. S. Bräse
Institute of Biological and Chemical Systems – Functional Molecular Systems (IBCS-FMS), Karlsruhe Institute of Technology (KIT), Kaiserstraße 12, 76131 Karlsruhe, Germany
E-mail: erem.ahmetali@kit.edu
stefan.braese@kit.edu

Dr. E. Ahmetali, Prof. S. Bräse
Institute for Biological Interfaces 3 (IBG-3) – Soft Matter Synthesis Laboratory (SML), Karlsruhe Institute of Technology (KIT), Kaiserstraße 12, 76131 Karlsruhe, Germany

Dr. E. Ahmetali
Department of Chemistry, Yıldız Technical University, Istanbul 34210, Turkey

Dr. A. Kocaarslan, S. Heißler
Institute for Functional Interfaces (IFG), Karlsruhe Institute of Technology (KIT), Kaiserstraße 12, 76131 Karlsruhe, Germany

V. Trouillet
Institute for Applied Materials – Energy Storage System (IAM-ESS), Karlsruhe Institute of Technology (KIT), Kaiserstraße 12, 76131 Karlsruhe, Germany

V. Trouillet
Karlsruhe Nano Micro Facility (KNMFi), Karlsruhe Institute of Technology (KIT), Kaiserstraße 12, 76131 Karlsruhe, Germany

Additional supporting information can be found online in the Supporting Information section

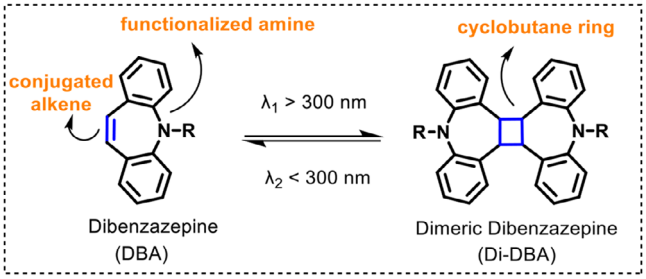

Figure 1. Reversible reaction of Dibenzazepine upon light irradiation above or below 300 nm.

conjugated alkene from the ground state into the excited singlet state, which is followed by intersystem crossing into the triplet state. The population of the triplet state can be increased by energy transfer from the excited photosensitizer (PS).[14–16] Dibenzazepine (DBA) is an aromatic compound that is commonly known for its biological activity[17,18] but it is capable of [2 + 2] photocycloaddition reactions due to the conjugated alkene in the structure.[19] It can undergo photodimerization upon light irradiation above 300 nm, resulting in cyclobutane ring while transforming to its original form below 300 nm wavelength.[20–22] DBA can be functionalized through its reactive secondary amine, and its dimeric derivatives can serve as a precursor for the synthesis of next-generation photodynamic macromolecules (Figure 1).

Heterogeneous photocatalysts (HPCs) are also strategic partners for recyclability and energy efficiency.[23,24] They play a crucial role in sustainable chemistry, energy conversion, and environmental remediation as they can be readily recovered from the reaction medium and activated photochemically.[25,26] Although traditional inorganic semiconductors such as TiO_2 and ZnO have been extensively employed as HPCs, ongoing research focuses on developing advanced strategies to diversify photocatalytic performance and extend light absorption into the visible spectrum.[27,28] The incorporation of convenient PSs into HPCs not only promotes the utilization of harmless and environmentally benign light sources, but also imparts distinctive functionalities.[29] PSs can facilitate many chemical and biological transformations by generating reactive species through energy or electron transfer to surrounding molecules.[30] The challenge lies in incorporating extended π-conjugated molecules into chemical architectures, as well as in overcoming the relatively low photon energy associated with the visible spectral region. The construction of covalent organic frameworks (COFs) and metal–organic frameworks (MOFs) is frequently employed for this purpose, necessitating the synthesis of multifunctional aromatic building blocks such as BODIPY[31] and porphyrin[32] derivatives. Among those structures, phthalocyanines (Pcs) stand out for their ability to exhibit strong absorption in the near-infrared (NIR) region, exceptional chemical and photochemical stability, and efficient triplet state population.[33,34] Molecular Pcs bearing multiple amine, hydroxyl, or anhydride substituents have also been successfully employed as building blocks in the synthesis of visible-light-responsive networks.[35,36] Nevertheless, despite their favorable photophysical and electronic properties, encouraging the integration of molecular Pcs into MOF and COF architectures has been confined owing to challenges associated with their efficient synthesis and derivatization.[37,38] Whereas mono-phthalonitrile derivatives are utilized in the synthesis of molecular Pcs, under the same conditions, bis-phthalonitrile derivatives constitute network polymeric phthalocyanines (NP-Pcs) in which organic structures serve as bridging units, significantly influencing the material's properties in conjunction with the central metal atom.[39–43] **NP-Pcs** represent a contemporary frontier in heterogeneous photocatalysis, offering more sustainable synthesis opportunities, facile purification, versatile functionality and efficient recyclability.[44,45] Even though a number of structures, including triethylene glycol,[46] spirobifluorene,[47] and naphthalene,[48] have served as bridging units in the construction of photocatalytic **NP-Pcs**, no photodynamic group has been investigated for this purpose.

Herein, we leverage photodynamic chemistry for the preparation of **NP-Pcs** as efficient degradable heterogeneous photocatalysts. Bis-phthalonitrile derivative incorporating the DBA dimer was synthesized through a light-induced [2 + 2] cycloaddition reaction at 368 nm, and this molecule was subsequently utilized as an organic bridge in the construction of network polymeric zinc and cobalt phthalocyanines (**NP-ZnPc** and **NP-CoPc**). The characterization of the **NP-Pcs** was completed by FTIR, Raman, UV–vis, TGA, XPS, and SEM measurements. Moreover, the soluble molecular Pcs, which were synthesized from mono phthalonitrile derivative, were also characterized by NMR and MALDI-TOF-MS to support the structure of **NP-Pcs**. The versatile functionality of the characterized photocatalysts was investigated under red light irradiation (630 and 647 nm). The singlet oxygen generation ability of **NP-Pcs** was evaluated by monitoring the photoreaction of diphenylisobenzofuran (DBF) via UV–vis spectroscopy. The formation of singlet oxygen has also been demonstrated in the oxidation reaction of methylphenyl sulfide, and the performance of photocatalysts has been tested in different conditions. Furthermore, detailed investigations have been conducted on the energy transfer properties of **NP-Pcs** during the PET-RAFT polymerization of 2-hydroxyethyl methacrylate (HEMA) monomer. Contribution with their heterogeneous nature, **NP-Pcs** were recovered after the polymerization and used up to three cycles without significant loss of performance. Notably, the end-of-life stage of materials has been achieved via the reversible nature of DBA, which allowed the controlled degradation under 254 nm light irradiation. This study constitutes the first reported example of **NP-Pcs** employing light irradiation for their "design, use and degradation".

Results and Discussion

Synthesis and Characterization of Molecular Phthalocyanines

The study focuses on the preparation of **NP-Pcs** bearing photodynamic DBA moiety in order to obtain degradable

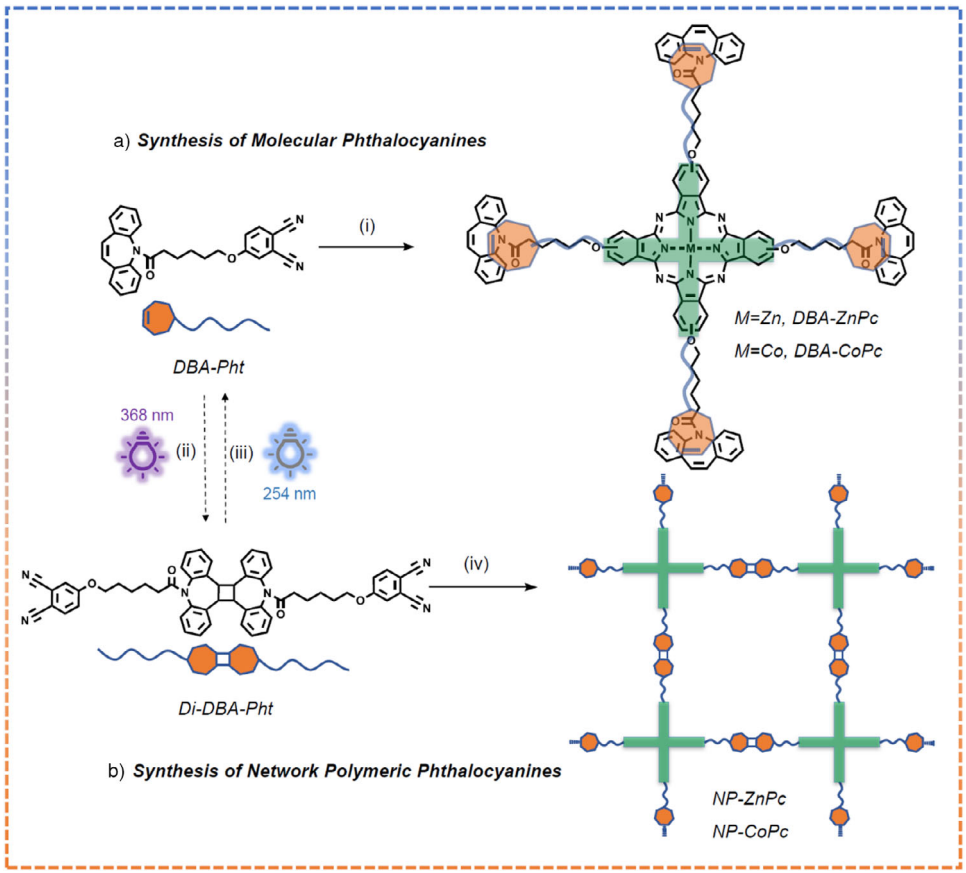

Figure 2. The synthesis scheme of a) molecular phthalocyanines and b) network polymeric phthalocyanines. i–iv) n-hexanol, DBU, zinc acetate or cobalt (II) chloride, 160 °C, 4 h ii) Acetone, n-hexane, benzophenone, 368 nm, 5 h iii) DCM, 254 nm, 2 h.

heterogeneous photocatalysts. Molecular Pcs were synthesized to evaluate the stability of DBA as a substituent and optimize the reaction conditions. First, DBA-functionalized phthalonitrile (**DBA-Pht**) was synthesized using 4-hydroxy phthalonitrile and bromine-substituted DBA (**DBA-Br**) in the presence of K_2CO_3 and DMF. Subsequently, the cyclotetramerization of the **DBA-Pht** was achieved in hexanol in the presence of DBU and corresponding metal salts, affording DBA-substituted phthalocyanines (**DBA-ZnPc** and **DBA-CoPc**) (Figure 2a). In the FTIR spectra, the nitrile (C ≡ N) stretching of **DBA-Pht** was observed at 2224 cm^{-1}, and this peak completely disappeared in **DBA-ZnPc** and **DBA-CoPc**. Moreover, the spectra showed aromatic C–H, aliphatic C–H, and C=O stretching at 3043 cm^{-1}, 2932 cm^{-1}, and 1663 cm^{-1}, respectively (Figures S1 and S2). While **DBA-Pht** does not display Raman activity, **DBA-ZnPc** and **DBA-CoPc** exhibit respective vibrations that support the characterization. The different electronic configurations of metal atoms give rise to vibrational frequency shifts for macrocycle C–N–C interactions. While ZnPc exhibits weaker interaction for C–N–C, CoPc has stronger metal–ligand orbital interactions, altering electron density distribution.[49] Nitrile (C ≡ N) stretching associated with the starting material was not observed, but C–N–C vibrations belonging to the Pc core appeared at 1501 cm^{-1} and 1534 cm^{-1} for Zn and Co derivatives, confirming effective cyclization reaction and influence of different metal ions (Figure S3).[50] In the evaluation of ^{1}H NMR spectra of **DBA-Br**, **DBA-Pht**, and **DBA-ZnPc**, the characteristic DBA double bond consistently appears at ~7.04 ppm. While aromatic protons of DBA were observed between 7.64 and 7.26 ppm (Figure S4), the phthalonitrile benzene appeared at 8.02 and 7.72 ppm (Figure S5). The cyclotetramerization of phthalonitrile into aromatic macrocyclic structure resulted in the observed shifts of these signals to 8.96 and 8.47 ppm (Figure S6). The characterization of **DBA-Pht**, **DBA-ZnPc**, and **DBA-CoPc** was supported by mass spectroscopy. In the MALDI-TOF-MS spectrum, exact mass values were observed at m/z 433.42, 1798.56, and 1793.09, respectively (Figure S9–S11). In addition, THF-SEC measurements were performed for **DBA-ZnPc** and **DBA-CoPc**, which resulted in uniform peaks. In particular, **DBA-ZnPc** exhibited a value of 1798.1, which exactly aligns with the expected result (Figure S12). UV–vis spectroscopy is a significant analytical technique for confirming the formation and presence of phthalocyanine derivatives. They have three characteristic absorption bands: i) the Q band found at 650–750 nm in the visible region, ii) the Q vibrational (Q_{vib}) band at 610–615 nm in the bluer region, and iii) the B (Soret) band observed at 300–350 nm in the ultraviolet region.[51] The UV–vis spectra of **DBA-ZnPc** exhibited these characteristic Pc bands at 677, 611, and 352 nm. Blue shift was observed for **DBA-CoPc**, and values were recorded as 665, 601,

and 333 nm arising from the different central metal ions (Figure S13).[52]

Dual Nature of Phthalonitrile-Substituted Dibenzazepine

The determination of the optimal reaction conditions for the formation of **NP-Pcs** was followed by the synthesis of their starting materials. **DBA-Pht** was irradiated at 368 nm in the presence of benzophenone in acetone-hexane mixture, and dimeric derivative **Di-DBA-Pht** was obtained (Figure 2a and b). The dimerization was confirmed through detailed analysis of proton (^{1}H) and carbon (^{13}C) NMR spectroscopy. The ^{1}H NMR spectrum revealed the characteristic cyclobutane protons at 3.80 ppm (Figure S14). Furthermore, combined analysis of the ^{13}C NMR and DEPT-135 spectra established that the resonance at 47.87 ppm belongs to the cyclobutane carbons (Figures S15 and S16). The structural characterization was also validated by MALDI-TOF-MS spectrometry, with the exact molecular mass recorded at m/z 866.27 (Figure S17).

Simultaneously, the reversible nature of **DBA-Pht** was investigated by ^{1}H NMR and UV-vis spectroscopy. Although a minor variation at 294 nm was observed in the UV-vis spectra due to spectral overlap with benzophenone during the dimerization reaction (Figure 3a), the ^{1}H NMR spectra clearly demonstrated the disappearance of the double bond at 7.04 ppm and the simultaneous appearance of the cyclobutane ring at 3.80 ppm (Figure 3b). The reversible reaction of **Di-DBA-Pht** was carried out in DCM under 254 nm light irradiation. Periodic sampling of the reaction mixture enabled detailed monitoring through UV-vis spectroscopy and ^{1}H NMR spectroscopy in DMSO. The initial heterogeneous mixture transitioned to a homogeneous solution, coinciding with the reformation of **DBA-Pht**. While the signal at 294 nm in the UV–vis spectrum increases dramatically (Figure 3c), the initial ^{1}H NMR spectrum of **DBA-Pht** was re-established (Figure 3d). Such bidirectional monitoring provides compelling evidence for the reversible photodynamic nature of **DBA-Pht**.

Synthesis and Characterization of Network Polymeric Phthalocyanines

After the successful synthesis of **Di-DBA-Pht, NP-ZnPc,** and **NP-CoPc** were prepared with the same synthetic conditions as molecular Pcs (Figure 2b). Due to their network structures, these materials are insoluble; hence, purification was achieved by sequential washing with multiple solvents. The characterization was achieved via solid-phase measurement in comparison with their starting material **Di-DBA-Pht**. The FTIR spectrum showed a characteristic C≡N stretching vibration at 2224 cm^{-1}; notably, this peak completely disappeared in the spectra of **NP-ZnPc** and **NP-CoPc**. Additional IR absorptions corresponding to aromatic C–H, aliphatic C–H, and C═O stretches were observed at 3043, 2932, and 1663 cm^{-1}, respectively (Figure 4a). In contrast to the **DBA-Pht**, the **Di-DBA-Pht** showed Raman activity, and the characteristic nitrile stretching was observed at 2227 cm^{-1}. The complete disappearance of the nitrile peak is clearly visible in the spectrum of **NP-ZnPc** and **NP-CoPc**. Moreover, distinct Raman C–N-C stretching vibrations belonging to **NP-ZnPc** and **NP-CoPc** were recorded at 1508 cm^{-1} and 1534 cm^{-1} (Figure 4b). All FTIR and Raman spectroscopic analyses have clearly indicated that **NP-Pcs** are compatible with the data of molecular Pcs. The absorbance spectra of **NP-Pcs** were measured using solid-state UV–vis spectroscopy (Figure 4c). The absorbance changes between 500 and 800 nm prove the transformation of **Di-DBA-Pht** to **NP-Pcs**. UV–vis spectra indicate that the synthesized **NP-Pcs** exhibit substantial absorbance maxima at 358, 620, and 679 nm in the ultraviolet and visible region, which belong to characteristic bands of Pcs.

The thermal stability of **Di-DBA-Pht**, **NP-ZnPc** and **NP-CoPc** was evaluated by thermogravimetric analysis (TGA) in the temperature range of 22–600 °C (Figure 4d). The decomposition temperatures of all investigated substances exceed 350 °C. This thermal value is significant because **Di-DBA-Pht** undergoes network formation at 160 °C. It shows that the cyclobutane ring stayed stable in the network architecture, whereas it is able to undergo rapid photodegradation under 254 nm light irradiation (Figure 3d). These findings offer compelling evidence that the reaction inaccessible under thermal conditions was achieved by photochemistry. All materials display a single thermal degradation peak; however, **NP-CoPc** shows a lower decomposition temperature (354.8 °C) compared to **Di-DBA-Pht** (380.4 °C) and **NP-ZnPc** (383.3 °C). This difference is attributed to the redox-active nature of cobalt, which reduces thermal stability at elevated temperatures.[53] Additionally, char yields were determined, representing the residual mass percentage after heating to 600 °C. Nearly complete degradation was observed for **Di-DBA-Pht** (6%), whereas approximately 40% of the **NP-Pcs** remained stable. This shows the superior thermal durability of the **NP-Pcs** (Table S1).

X-ray photoelectron spectroscopy (XPS) analyses were systematically conducted on **Di-DBA-Pht** and **NP-Pcs** to provide detailed insights into their elemental composition and the chemical environment of the different elements. The XPS survey spectra distinctly illustrated the elemental compositions of the network structures (Figure 4e). Detailed investigation of the high-resolution N 1 s spectra revealed notable differences between **Di-DBA-Pht** and **NP-Pcs** (Figure 4f). **Di-DBA-Pht** exhibited a singular peak at 399.7 eV, indicating nitrogen atoms in amide (N–C═O) and nitrile (C≡N) environments. However, the **NP-Pcs** displayed two clearly distinguishable nitrogen-related signals at 400.1 and 398.5 eV. To accurately assign these observed peaks, comparative XPS measurements were performed on standard references: unsubstituted metal-free phthalocyanine (H_2Pc) as well as ZnPc and CoPc. Reference data indicated two distinct peaks for the H_2Pc, whereas both ZnPc and CoPc exhibited a single consolidated peak at approximately 398.9 eV. These results suggest that both the pyrrolic and bridging nitrogen atoms are equally influenced by the presence of the metal center, which leads to only one binding energy. Based on these findings, the peak at 398.5 eV in the

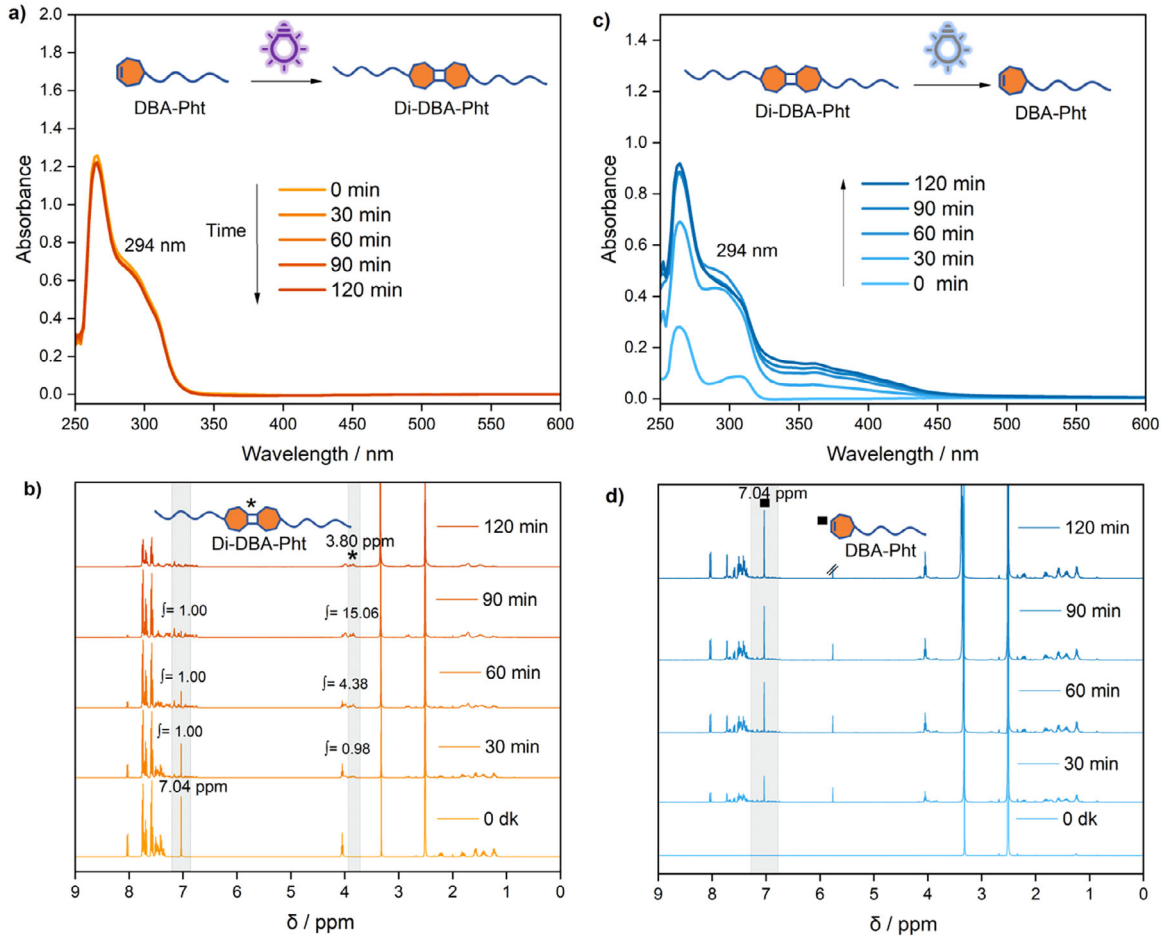

Figure 3. The spectroscopic evaluation of the reversible nature of **DBA-Pht** in DMSO a) UV–vis screening of dimerization upon 368 nm light exposure b) ^{1}H NMR changes of dimerization c) UV–vis screening of cleavage upon 254 nm light exposure d) ^{1}H NMR changes of cleavage.

NP-Pcs can be attributed to the Pcs nitrogen atoms, while the other at 400.1 eV corresponds to the nitrogen atoms of the DBA units. Analysis of the C 1 s spectra further supported the structural assignments, showing four distinct carbon environments. The peak at 285.0 eV corresponded to C–C, C–H, and C═C carbon atoms, reflecting their dominance within the molecular structure. Signals at 286.5 eV are attributed to C–O and C–N, while a higher binding energy at 287.9 eV was associated with strongly electron-withdrawing functionalities: C═O, C═N, and C≡N groups. In addition, the $\pi \rightarrow \pi^*$ transition, which is the characteristic excitation peak for aromatic structures, was detected at 291.6 eV as a broad, weak signal (Figure S18a). Complementary O 1 s spectra validated these species attributions, identifying distinct oxygen environments at 532.9 eV (C–O functionality) and 531.3 eV (C═O functionality) (Figure S18b). The determination of the binding energies of zinc (Zn) and cobalt (Co) is crucial to demonstrate that Zn and Co metal ions coordinate to the Pc donor atoms and form extended two- or 3D NP-Pc architectures. Zn displayed its distinctive 2p dublet at 1021.6 and 1044.3 eV, corresponding to Zn $2p_3/_2$ and Zn $2p_1/_2$ states, while Co was confirmed via photoelectron lines at binding energies of 780.8 eV and 796.5 eV for the respective (Co $2p_3/_2$) and (Co $2p_1/_2$) states (Figure S18c, S18d). These results align closely with literature values, reinforcing the compositional interpretation of the **NP-Pcs**.[54–56] SEM analysis of **NP-Pcs** reveals heterogeneous, porous morphologies with interconnected domains, reflecting the extended network structure.[46,57] The SEM images of **NP-ZnPc** and **NP-CoPc** exhibit irregular aggregates with a fibrous texture, consistent with network formation (Figure 4g and h).

Singlet Oxygen Generation Efficiency

DBA unit in the present concept is incorporated as a covalently linked DBA dimer within a network architecture, rather than as an isolated, conjugated chromophore. In this configuration, the DBA dimer functions as a rigid, non-conjugated bridge connecting Pcs units via flexible aliphatic spacers and ester linkages. This structural motif limits electronic communication between the DBA dimer and the Pc macrocycles. Moreover, the low-lying triplet excited state of the Pc core lies significantly below the excited-state energies expected for DBA-based aromatic amines, rendering triplet energy transfer from the Pc to the DBA dimer thermodynamically unfavorable.[58,59] Therefore, the DBA dimer bridge primarily serves as a structural and degradable

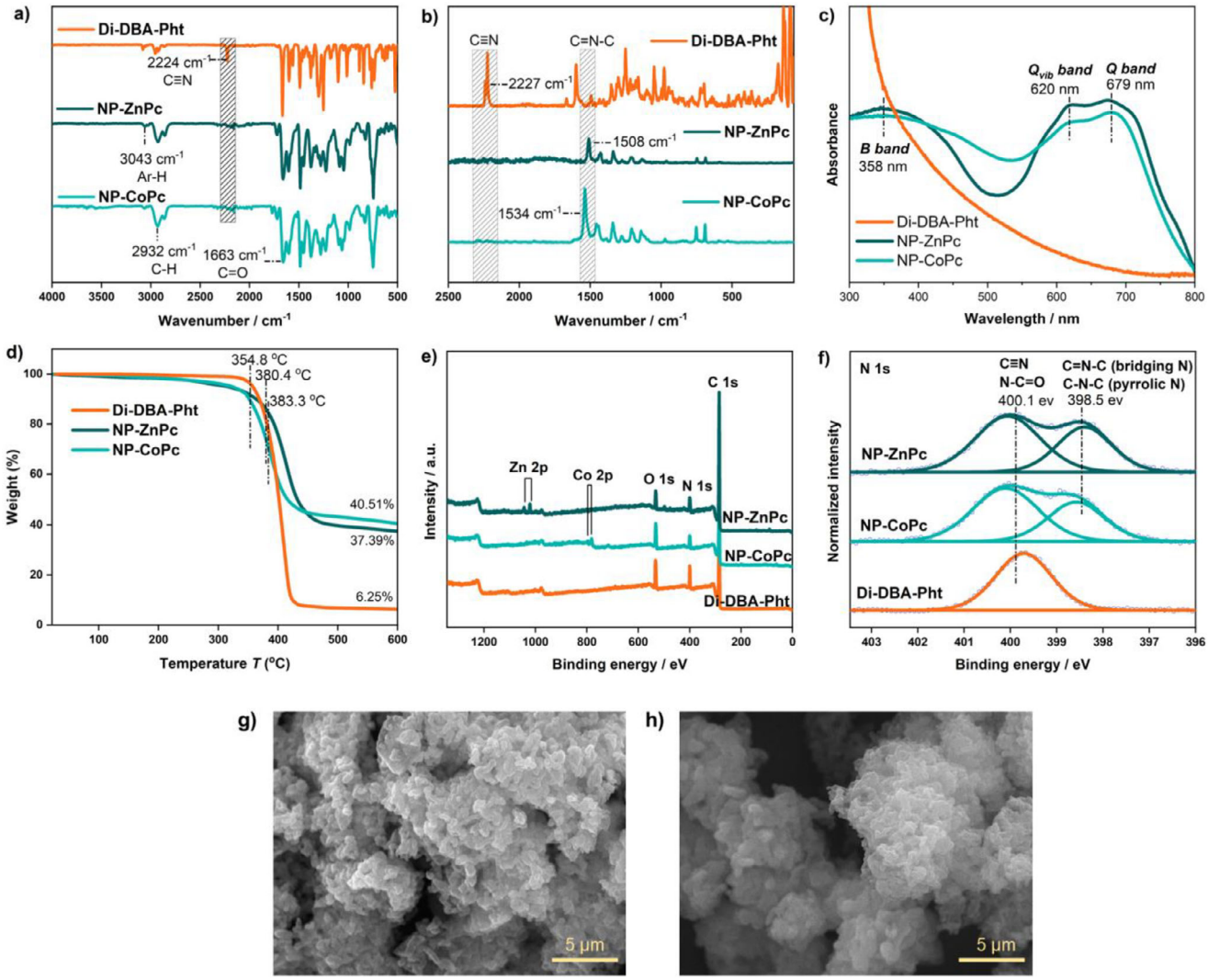

Figure 4. a) FT-IR spectra b) Raman spectra c) Solid state UV–vis spectra d) TGA curves e) XPS survey spectra f) N 1 s XPS spectra of **Di-DBA-Pht**, **NP-ZnPc,** and **NP-CoPc** g) SEM image of **NP-ZnPc** h) SEM image of **NP-CoPc**.

linker, while photocatalytic activity is dominated by the Pc units.

Pcs are well-known for their efficient intersystem crossing, attributed to their highly conjugated aromatic framework, and the presence of heavy metal centers.[60] Upon excitation to the triplet state, these compounds can facilitate the generation of reactive singlet oxygen species from molecular oxygen, enabling versatile ability in many applications such as photodynamic therapy against cancer cells[61] and pathogenic microorganisms,[62] as well as organic transformations[63] (Figure 5a). The singlet oxygen generation capability of **NP-ZnPc** and **NP-CoPc** was evaluated in DMF via UV–vis spectroscopy using DPBF as a chemical quencher. DPBF undergoes a structural transformation upon reaction with singlet oxygen, resulting in a progressive decrease in its absorbance around 415 nm. It is known that the rate of the decrease is directly correlated with the efficiency of singlet oxygen production. **NP-ZnPc** and **NP-CoPc** (0.5 mg/mL) were mixed with an equal amount of DPBF (~1.3 a.u.) and sonicated to ensure dispersion. The samples were irradiated with red light (630 nm, 4.72 mW/cm^2) at short time intervals, and the absorbance changes were monitored (Figure S19a and b). While both **NP-Pcs** demonstrated singlet oxygen generation, **NP-ZnPc** exhibited a markedly higher efficiency, leading to a rapid quenching of DBF absorbance (from 1.3 a.u. to 0.2 a.u. in 30 s). It is also observed that there is no change in the characteristic Q-band (~680 nm) of the **NP-Pcs**. This shows that the **NP-Pcs** indicated good photostability and structural integrity under these conditions.

Sulfoxides are widely applied in organic synthesis and bioactive ingredients in the pharmaceutical industry. Although plenty of protocols have been developed for the efficient synthesis of sulfoxides from sulfides, aerobic photo-oxidation is the most straightforward and green pathway because it utilizes light energy and oxygen instead of expensive or toxic materials.[64] Owing to its high energy and absence of spin restriction, singlet oxygen is recognized as a powerful tool for oxidation of sulfides.[65] In the supporting experiments, the production of singlet oxygen via **NP-Pcs** has been confirmed through an oxidation reaction

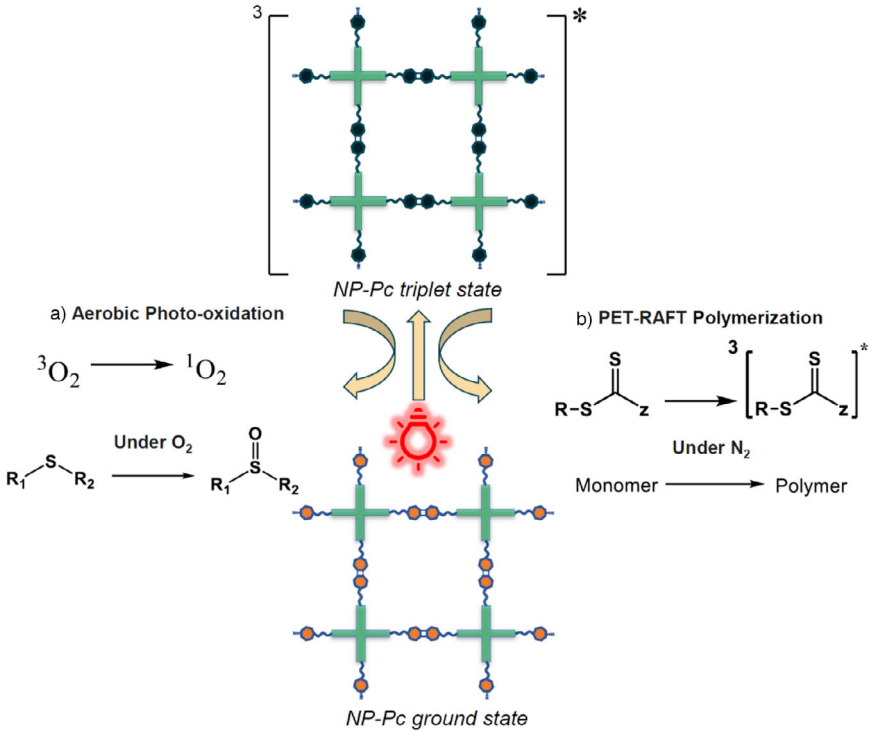

Figure 5. Simplified functionality mechanism of **NP-Pcs** a) Aerobic Photo-oxidation b) PET-RAFT polymerization.

Table 1: Different conditions for photo-oxidation of methylphenyl sulfide.

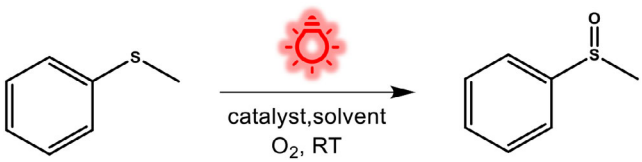

Entry[a]	Catalyst	Solvent	Time (h)	Conv[b] (%)
1	NP-CoPc	MeCN / MeOH (1:1)	7	0
2	NP-CoPc	MeCN / MeOH (1:1)	24	0
3	NP-ZnPc	MeCN / MeOH (1:1)	18	36
4	NP-ZnPc	MeCN / MeOH (1:1)	24	59
5	NP-ZnPc	MeCN	17	0
6	NP-ZnPc	MeCN	24	0
7	NP-ZnPc	DMSO	6	13
8	NP-ZnPc	DMSO	24	60
9	NP-ZnPc	MeOH	9	21
10	NP-ZnPc	MeOH	24	59
11	NP-ZnPc	MeOH	2	79[c]
12	NP-ZnPc	MeOH	4	100[c]

[a] Conditions: Methylphenyl sulfide (0.5 mmol) catalyst (5 mg) in 4 mL solvent with O_2 atmosphere under 630 nm red light irradiation (4.72 mW/cm^2) at room temperature. [b] Determined by ^{1}H NMR. [c] under 647 nm red light irradiation (12.94 mW/cm^2).

of methylphenyl sulfide under red light irradiation. The efficiency of oxidation was monitored by ^{1}H NMR spectroscopy (Figure S20). The reaction yields of **NP-ZnPc** and **NP-CoPc** are summarized in Table 1 for different solvents, times, and light intensity. 100% efficiency was achieved with **NP-ZnPc** in methanol, whereas no conversion was observed for **NP-CoPc**. **NP-ZnPc** has reached roughly similar yields in many solvents except acetonitrile, which has relatively low oxygen solubility compared to MeOH or DMSO and a much shorter singlet oxygen lifetime.[66] The superior performance of **NP-ZnPc** can be attributed to its diamagnetic nature, which facilitates intersystem crossing and stabilizes the triplet state population, whereas the paramagnetic **NP-CoPc** tends to quench excited states more rapidly, reducing its triplet sensitization efficiency.[67]

PET-RAFT Polymerization Initiated by Network Polymeric Phthalocyanines

Pcs are also famous photosensitizers capable of initiating polymerization reactions by transferring their excited-state energy to neighboring molecules. In the presence of a chain transfer agent (CTA), initiation can be controlled to achieve well-defined polymers with narrow molecular weight distributions (Figure 5b).[68,69] Photoinduced electron or energy transfer reversible addition fragmentation chain transfer (PET-RAFT) is a photocontrolled polymerization technique that frequently employs thiocarbonylthio compounds as CTAs.[70] Within the study, we investigated the polymerization of 2-hydroxyethyl methacrylate (HEMA) in the presence of **NP-Pcs** using a trithiocarbonate derivative as CTA upon red-light exposure (647 nm, 12.94 mW/cm^2). DMSO was employed as a solvent to facilitate the efficient dispersion of the heterogeneous catalysts. While 96%

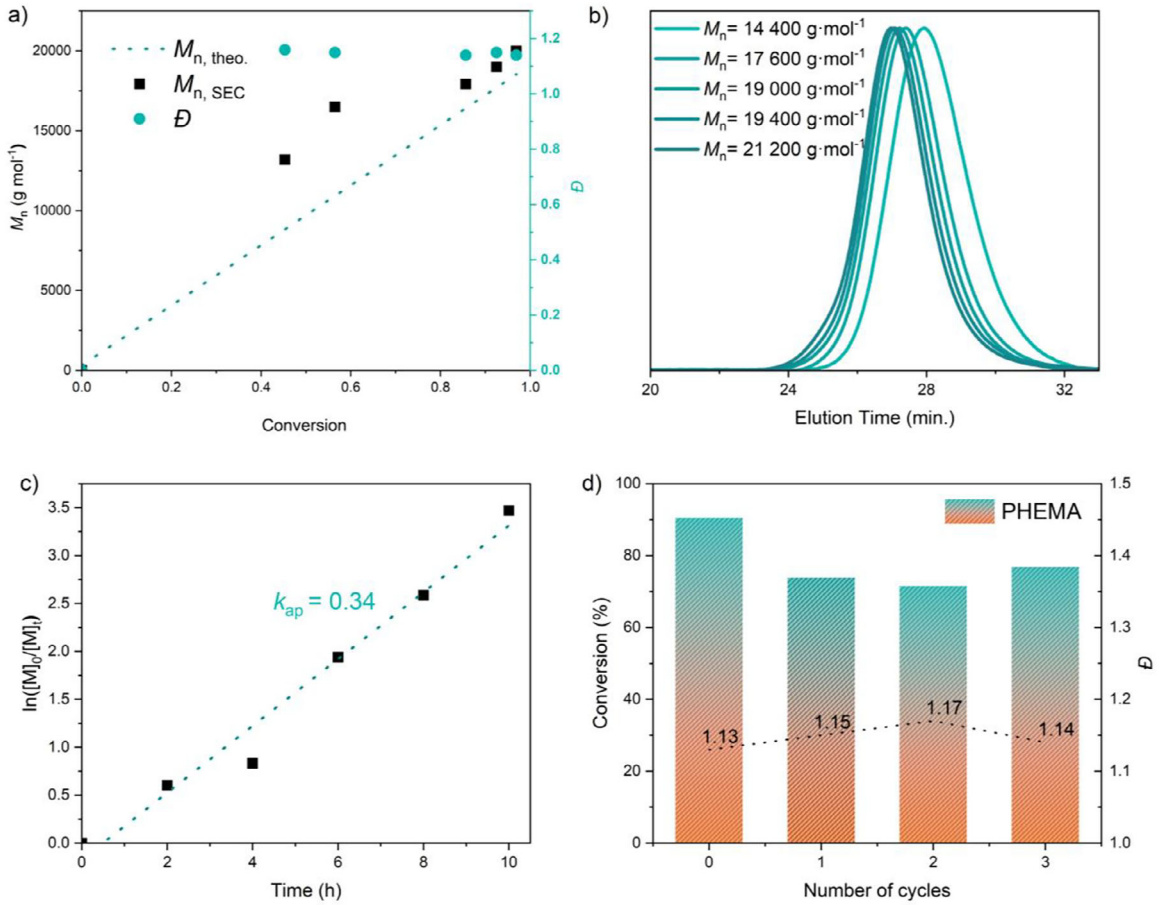

Figure 6. Kinetic evaluation of PET-RAFT polymerization of HEMA under red light irradiation (647 nm, 12.94 mW/cm^2) a) Number-average molar mass ($M_{n,SEC}$) and molar mass dispersity (Đ) as a function of monomer conversion b) In situ SEC traces of the resulting polymers during PET-RAFT polymerization of HEMA c) Evolution of $\ln([M]_0/[M]_t)$ as a function of time d) Recycling performance of **NP-ZnPc** as a heterogeneous photocatalyst over multiple cycles.

monomer conversion was achieved within 10 h in the presence of the **NP-ZnPc**, by contrast, no polymer formation was detected in control experiments either in the absence of photocatalyst (blank) or in the presence of **NP-CoPc**. It shows that **NP-ZnPc** is actually an efficient photocatalyst for PET-RAFT while **NP-CoPc** is essentially "dark" for this purpose. These findings are consistent with the results obtained for singlet oxygen generation and collectively substantiate the efficiency of triplet-state energy transfer. Strong contrast in activity between **NP-ZnPc** and **NP-CoPc** highlights the critical role of the central metal ion in modulating the photophysical properties of the macrocycle structures.

The PET-RAFT polymerization kinetics of **NP-ZnPc** (4.2 mg) were investigated under constant reaction conditions with an initial ratio of $[HEMA]_0/[TTC]_0 = 113/1$ (Figure S21). While monomer conversion of 45% was achieved in 2 h, it reached to 96% end of the 10 h reaction time. Over this period, the number-average molecular weight (M_n) increased linearly from 14400 to 21200 g·mol^{-1}, whereas the molecular weight distribution remained constant (Đ = ~1.15), which strongly indicates the features of a living nature of PET-RAFT polymerization (Figure 6a and b). The instantaneous change in monomer concentration was further evaluated by semi-logarithmic analysis (Figure 6c). A linear correlation of $\ln([M]_0/[M]_t)$ with irradiation time (t) was observed, corresponding to first-order kinetics with an apparent rate constant of k_{app} (647 nm) = 0.34 h^{-1}. Another distinctive characteristic of **NP-Pcs** is their heterogeneous nature. Unlike homogeneous photocatalysts, they are insoluble, resist photolysis, and therefore, they are environmentally friendly molecules that can be recovered and reused. To assess their recyclability, PET-RAFT polymerizations were performed with **NP-ZnPc** until three consecutive cycles (Figure 6d). Although a slight reduction in monomer conversion was observed after the first cycle, subsequent cycles showed high performance (~75% conversion) together with the consistent dispersity values (~1.15). Notably, post characterization data of the **recycled NP-ZnPc** provides strong evidence for the structural integrity and sustainable catalytic activity (Figure S22).

Photodegradation of Network Polymeric Phthalocyanines

Following confirmation of their functionality, the final step involves investigating the photodegradation behavior of the **NP-Pcs**. This step is essential, as although DBA contributes

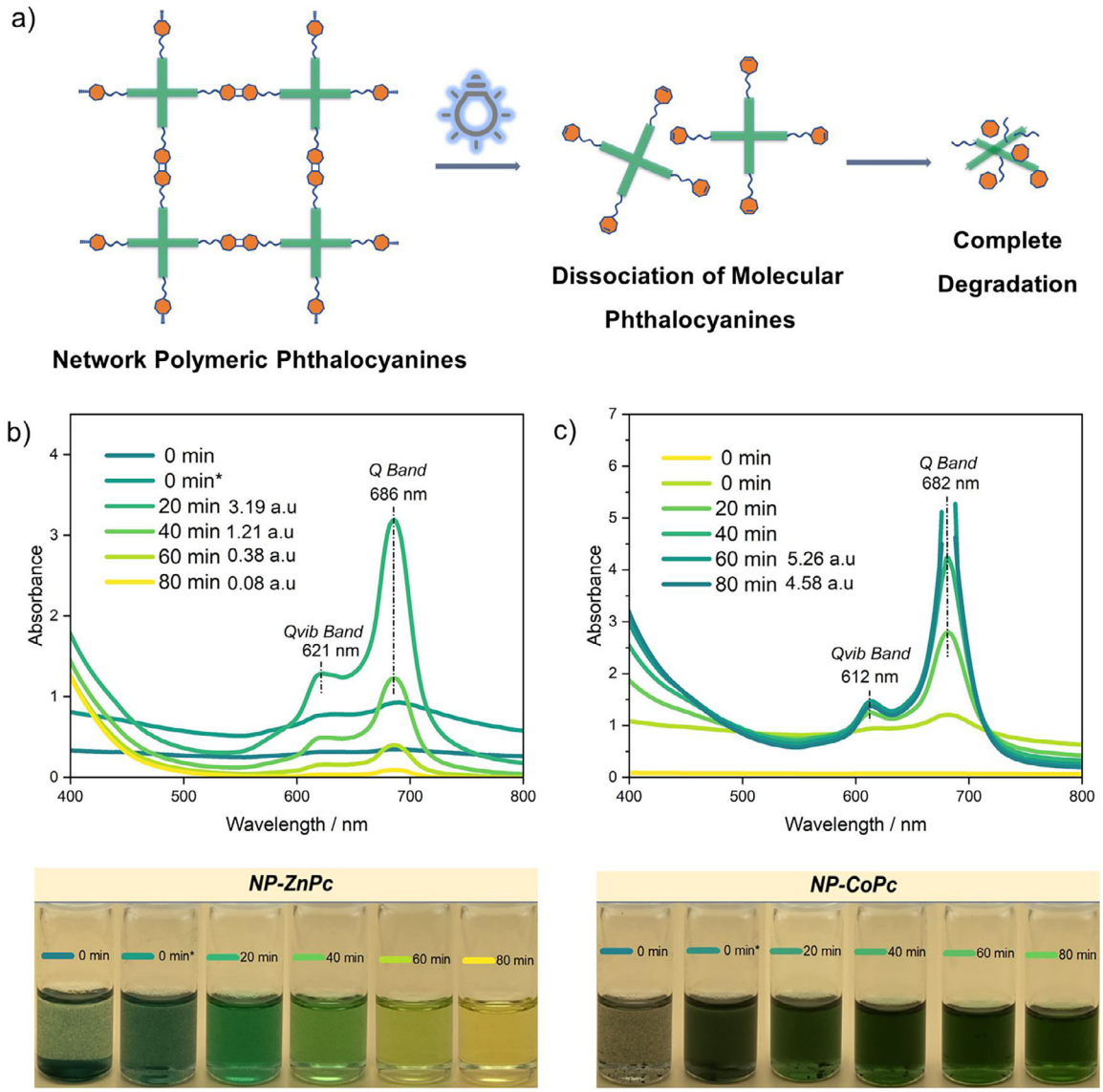

Figure 7. a) Proposed photodegradation path of network polymeric phthalocyanines b) absorbance changes of **NP-ZnPc** c) absorbance changes of **NP-CoPc** under 254 nm light irradiation in DMSO.

additional characteristics to the network—such as aromaticity and the heteroatoms—its primary role is to provide degradability to the **NP-Pcs**. Experimental investigations on the reversible behavior of **Di-DBA-Pht** have demonstrated that irradiation with 254 nm light provides successful cleavage of the cyclobutane ring, regenerating the conjugated alkene bonds (Figure 3c and d). Therefore, it is expected that exposure of the **NP-Pcs** to the same irradiation leads to the dissociation of molecular Pcs and subsequent degradation (Figure 7a). For this purpose, 0.5 mg/mL **NP-Pcs** suspensions in DMSO were dispersed in ultrasonic bath for 5 min and exposed to 254 nm light irradiation. All changes were monitored via visual observations, UV–vis, MALDI-TOF-MS, and ^{1}H NMR spectroscopy. The heterogeneity in both networks was replaced by homogeneity over time, and all solid particles were dissolved. In the case of the **NP-ZnPc**, dissociation was observed within the first 20 min, and absorbance reached a maximum value (3.2 a.u.). Subsequently, degradation has begun and is followed by a loss of characteristic Pc color and a sharp decrease in absorbance (Figure 7b). However, **NP-CoPc** exhibited a slower degradation in comparison with **NP-ZnPc**. Absorbance value gradually increased until reaching a maximum of 5.2 a.u. in 60 min, while protecting its color. Degradation commenced after this point, as evidenced by a subsequent decrease in absorbance (Figure 7c). The comparatively slower degradation of the cobalt derivative can be derived from the redox-active nature, which can interact with photogenerated radicals or excited states, thereby quenching active species and delaying the degradation process. [71] As a further consideration, MALDI-TOF-MS and ^{1}H NMR spectroscopy were performed at 20 min of irradiation for **NP-ZnPc**, and 60 min for **NP-CoPc**. In the MALDI-TOF-MS spectra, signals corresponding to **DBA-ZnPc** and **DBA-CoPc** were detected at m/z 1802 $[M + 4H]^+$ and 1795 $[M + 2H]^+$,

respectively. Consistently, the ^{1}H NMR spectra revealed the reappearance of the characteristic DBA double bond at 7.02 ppm, along with the expected aromatic resonances, confirming the reversible reaction of photodynamic linkage (Figure S23).

Conclusion

In this study, dibenzazepine (DBA) photodynamic molecule was incorporated into a **NP-Pc** to obtain degradable heterogeneous photocatalyst. First, DBA-substituted phthalonitrile (**DBA-Pht**) was synthesized and utilized in the synthesis of molecular zinc and cobalt phthalocyanines (**DBA-ZnPc** and **DBA-CoPc**) to validate the compatibility of DBA substituent on the Pc structure. Then, Dimer of the **DBA-Pht** (**Di-DBA-Pht**) was synthesized through [2 + 2] photocycloaddition reaction under 368 nm light irradiation. TGA revealed that **Di-DBA-Pht** exhibits remarkable thermal stability up to high temperatures (380.4 °C), while demonstrating reversible photochemical cleavage under 254 nm light irradiation. Accordingly, the preparation of **NP-ZnPc** and **NP-CoPc** has been achieved by subjecting the dimer to the reaction conditions previously optimized for molecular Pcs. FTIR and Raman analyses confirmed the successful conversion of nitrile functionalities into imine bonds, and the characteristic Q-band at 679 nm in the UV–vis spectra indicated successful cyclotetramerization. XPS survey scans supported the elemental composition (C, N, O, Zn, or Co) of the structures and notably identified distinct nitrogen binding energies associated with the DBA (400.1 eV) and the Pc core (398.4 eV). Following structural characterization, the photoactivity of the **NP-Pcs** was evaluated through singlet oxygen generation and photopolymerization experiments. Bleaching of DPBF was followed by UV–vis spectroscopy, indicating singlet oxygen production upon red light (λ = 630 nm) irradiation. In particular, **NP-ZnPc** almost completely quenched the DPBF absorbance within 30 s, consistent with the high efficiency reported for zinc Pcs in the literature. The singlet oxygen-generating ability was also tested in the oxidation of sulfides. Methylphenyl sulfide was successfully converted to the corresponding sulfoxide derivative through **NP-ZnPc** with 100% yields in methanol. **NP-ZnPc** further demonstrated its superior performance in photoinduced electron/energy transfer-reversible addition–fragmentation chain transfer (PET-RAFT) polymerization under red-light irradiation (λ = 647 nm). In the presence of a chain transfer agent, the polymerization reached 96% conversion of 2-hydroxyethyl methacrylate within 10 h, affording poly(2-hydroxyethyl methacrylate) with a number-average molecular weight of 21,200 g mol^{-1} and a narrow molecular weight distribution (Đ) value of 1.15. Kinetic analysis at 2 h intervals revealed that a linear increase in molecular weight (14400–21200 g/mol) and a steady decrease in monomer concentration ($\ln([M]_0/[M]_t$ = 0.6–3.4) reflected the living characteristics of PET-RAFT polymerization. After polymerization reactions, the heterogeneous **NP-ZnPc** was recovered and reused for up to three consecutive cycles. The negligible decline after the first cycle was followed by an average of ~75% monomer conversion together with the consistent dispersity values (~1.15). The emerging concept of material science, functionality is no longer sufficient; beyond performance and recyclability, the end-of-life of materials has also become critical for achieving more sustainability. The reversible nature of the DBA enabled the degradation opportunity of the **NP-Pcs** upon exposure to 254 nm light irradiation in DMSO. Whereas the **NP-ZnPc** undergoes complete degradation within 80 min, **NP-CoPc** exhibits a slower degradation profile. The completion of the "design-use-degradation" cycle not only makes this study more sustainable in terms of the material design, but also shows that it contains an environmentally friendly approach by utilizing light energy, reusable, and degradable heterogeneous photocatalysts. We believe that this work can serve as a conceptual and practical milestone in the development of a new generation functional and degradable macromolecules leveraging photodynamic chemistry.

Acknowledgements

E.A. would like to acknowledge the financial support of the European Union under the name of Marie Skłodowska Curie Actions (Project number: 101150270). Authors also would like to thank Frank Kirschhöfer, Matthias Schwotzer, Alexei Kiselev for MALDI-TOF-MS, SEM, and BET analysis. E.A. would like to thank Patrick Hodapp and Birgit Huber for their valuable contributions. A.K. is thankful for the Liebig Fellowship supported by the German Chemical Industry (VCI). All authors would like to acknowledge the Ministry of Science, Research, and the Arts of Baden-Württemberg (MWK), Germany's Excellence Strategy 2082/1–390761711 (Excellence Cluster "3D Matter Made to Order"), as well as the Helmholtz Association for the financial support provided during the research.

Open access funding enabled and organized by Projekt DEAL.

Conflict of Interests

The authors declare no conflict of interest.

Data Availability Statement

Data that refers to the experiments described herein were submitted to the repository Chemotion (https://www.chemotion-repository.net/). All DOIs minted for the data are linked in the SI. New data obtained in this study is assigned to the collection embargo number EAA_2025-01-14 (https://doi.org/10.14272/collection/EAA_2025-01-14).

Keywords: Dibenzazepine · Heterogeneous photocatalysts · Network polymeric phthalocyanine · Photodynamic covalent bond

[1] A. Chennak, K. Giannakas, T. Awada, *Circ. Econ. and Sustain.* **2024**, *4*, 3007–3023, https://doi.org/10.1007/s43615-023-00297-8.
[2] N. Singh, T. R. Walker, *npj Mater. Sustain.* **2024**, *2*, 17, https://doi.org/10.1038/s44296-024-00024-w.
[3] D. Peti, J. Dobránsky, P. Michalík, *Polymers* **2025**, *17*, 603, https://doi.org/10.3390/polym17050603.
[4] R. Geyer, J. R. Jambeck, K. L. Law, *Sci. Adv.* **2017**, *3*, e1700782.
[5] X. Lin, J. Wang, B. Ding, X. Ma, H. Tian, *Angew. Chem. Int. Ed.* **2021**, *60*, 3459–3463, https://doi.org/10.1002/anie.202012298.
[6] P. Chakma, D. Konkolewicz, *Angew. Chem. Int. Ed.* **2019**, *58*, 9682–9695, https://doi.org/10.1002/anie.201813525.
[7] Y. Guo, C. Luo, M. Yang, H. Wang, W. Ma, K. Hu, L. Li, F. Wu, R. Chen, *Angew. Chem.* **2024**, *136*, e202406597.
[8] L. T. Nguyen, S. Maes, F. E. Du Prez, *Adv. Funct. Mater.* **2025**, *35*, 2419240, https://doi.org/10.1002/adfm.202419240.
[9] Y. Huang, X. Zheng, J. Wu, Y. Gao, Q. Ling, Z. Lin, *Nat. Commun.* **2024**, *15*, 6514, https://doi.org/10.1038/s41467-024-50943-4.
[10] W. Zou, B. Jin, Y. Wu, H. Song, Y. Luo, F. Huang, J. Qian, Q. Zhao, T. Xie, *Sci. Adv.* **2020**, *6*, eaaz2362, https://doi.org/10.1126/sciadv.aaz2362.
[11] V. X. Truong, C. Barner-Kowollik, *Trends in Chem.* **2022**, *4*, 291–304, https://doi.org/10.1016/j.trechm.2022.01.011.
[12] M. Li, A. Pal, A. Aghakhani, A. Pena-Francesch, M. Sitti, *Nat. Rev. Mater.* **2022**, *7*, 235–249, https://doi.org/10.1038/s41578-021-00389-7.
[13] K. Kalayci, H. Frisch, V. X. Truong, C. Barner-Kowollik, *Nat. Commun.* **2020**, *11*, 4193, https://doi.org/10.1038/s41467-020-18057-9.
[14] G. Kaur, P. Johnston, K. Saito, *Polym. Chem.* **2014**, *5*, 2171–2186, https://doi.org/10.1039/C3PY01234D.
[15] H. Frisch, D. E. Marschner, A. S. Goldmann, C. Barner-Kowollik, *Angew. Chem. Int. Ed.* **2018**, *57*, 2036–2045, https://doi.org/10.1002/anie.201709991.
[16] S. Poplata, A. Tröster, Y.-Q. Zou, T. Bach, *Chem. Rev.* **2016**, *116*, 9748–9815, https://doi.org/10.1021/acs.chemrev.5b00723.
[17] K. K. Katyayan, Y.-H. Hui, *Xenobiotica* **2019**, *49*, 1458–1469, https://doi.org/10.1080/00498254.2019.1572938.
[18] K. S. V. Kumar, G. S. Lingaraju, Y. K. Bommegowda, A. C. Vinayaka, P. Bhat, C. S. P. Kumara, K. S. Rangappa, D. C. Gowda, M. P. Sadashiva, *RSC Adv.* **2015**, *5*, 90408–90421, https://doi.org/10.1039/C5RA17926B.
[19] A. K. Alimoglu, C. H. Bamford, A. Ledwith, Y. Yagci, *Die Makromol. Chem.* **1992**, *193*, 1551–1556, https://doi.org/10.1002/macp.1992.021930630.
[20] J. Querner, D. Scheller, T. Wolff, *J. Photochem. Photobiol. A Chem.* **2002**, *150*, 85–91, https://doi.org/10.1016/S1010-6030(02)00034-5.
[21] J. Querner, T. Wolff, H. Görner, *Chem.–A Eur. J.* **2004**, *10*, 283–293, https://doi.org/10.1002/chem.200305199.
[22] S. Bener, C. Aydogan, Y. Yagci, *Macromol. Rapid Commun.* **2020**, *41*, 2000369, https://doi.org/10.1002/marc.202000369.
[23] M. Rudra, T. Bhowmik, H. Tripathi, R. Kumar, R. Sutradhar, T. Sinha, *Phys. B* **2021**, *619*, 413213, https://doi.org/10.1016/j.physb.2021.413213.
[24] A. Kocaarslan, Z. Eroglu, G. Yilmaz, O. Metin, Y. Yagci, *ACS Macro Lett.* **2021**, *10*, 679–683, https://doi.org/10.1021/acsmacrolett.1c00298.
[25] G. Messire, E. Caillet, S. Berteina-Raboin, *Catalysts* **2024**, *14*, 593, https://doi.org/10.3390/catal14090593.
[26] J. Chen, J. Cen, X. Xu, X. Li, *Catal. Sci. Technol.* **2016**, *6*, 349–362, https://doi.org/10.1039/C5CY01289A.
[27] A. Baig, M. Siddique, S. Panchal, *Catalysts* **2025**, *15*, 100.
[28] G.-Z. Li, S. Zhang, D. Tian, G. Liu, W. Wang, G. Chen, J. Wang, W. Wan, C. Yang, H. Yu, *Catal. Lett.* **2024**, *154*, 3896–3910, https://doi.org/10.1007/s10562-024-04622-0.
[29] M. Lu, S. B. Zhang, M. Y. Yang, Y. F. Liu, J. P. Liao, P. Huang, M. Zhang, S. L. Li, Z. M. Su, Y. Q. Lan, *Angew. Chem.* **2023**, *135*, e202307632.
[30] D. Kim, V. Q. Dang, T. S. Teets, *Chem. Sci.* **2024**, *15*, 77–94, https://doi.org/10.1039/D3SC04580C.
[31] T. Naranjo, L. Collado, M. Gomez-Mendoza, A. H. Pizarro, M. Barawi, F. Gándara, M. Liras, V. A. de la Peña O'Shea, *ACS Catal.* **2024**, *14*, 283–291, https://doi.org/10.1021/acscatal.3c04464.
[32] G. Lin, H. Ding, R. Chen, Z. Peng, B. Wang, C. Wang, *J. Am. Chem. Soc.* **2017**, *139*, 8705–8709, https://doi.org/10.1021/jacs.7b04141.
[33] E. Ahmetali, A. Kocaarslan, S. Bräse, P. Théato, M. K. Şener, *Macromol. Rapid Commun.* **2025**, *46*, 2400601, https://doi.org/10.1002/marc.202400601.
[34] E. Nikoloudakis, I. López-Duarte, G. Charalambidis, K. Ladomenou, M. Ince, A. G. Coutsolelos, *Chem. Soc. Rev.* **2022**, *51*, 6965–7045, https://doi.org/10.1039/D2CS00183G.
[35] B. Mishra, A. Alam, A. Chakraborty, B. Kumbhakar, S. Ghosh, P. Pachfule, A. Thomas, *Adv. Mater.* **2025**, *37*, 2413118, https://doi.org/10.1002/adma.202413118.
[36] B. Han, X. Ding, B. Yu, H. Wu, W. Zhou, W. Liu, C. Wei, B. Chen, D. Qi, H. Wang, *J. Am. Chem. Soc.* **2021**, *143*, 7104–7113, https://doi.org/10.1021/jacs.1c02145.
[37] E. L. Spitler, W. R. Dichtel, *Nat. Chem.* **2010**, *2*, 672–677, https://doi.org/10.1038/nchem.695.
[38] Z. Meng, R. M. Stolz, K. A. Mirica, *J. Am. Chem. Soc.* **2019**, *141*, 11929–11937, https://doi.org/10.1021/jacs.9b03441.
[39] A. W. Snow, J. R. Griffith, N. Marullo, *Macromolecules* **1984**, *17*, 1614–1624, https://doi.org/10.1021/ma00138a033.
[40] N. B. McKeown, *J. Mater. Chem.* **2000**, *10*, 1979–1995, https://doi.org/10.1039/b000793p.
[41] A. Gürek, Ö. Bekaroğlu, *J. Porphyrins Phthalocyanines* **1997**, *1*, 227.
[42] H. Yurtseven, M. A. Kaya, A. Altındal, M. K. Şener, *Des. Monomers Polym.* **2014**, *17*, 58–68, https://doi.org/10.1080/15685551.2013.840468.
[43] Y. Kim, D. Kim, J. Lee, L. Y. S. Lee, D. K. Ng, *Adv. Funct. Mater.* **2021**, *31*, 2103290, https://doi.org/10.1002/adfm.202103290.
[44] H. J. Mackintosh, P. M. Budd, N. B. McKeown, *J. Mater. Chem.* **2008**, *18*, 573–578, https://doi.org/10.1039/B715660J.
[45] N. B. McKeown, S. Makhseed, P. M. Budd, *Chem. Commun.* **2002**, 2780–2781, https://doi.org/10.1039/b207642j.
[46] J. Sun, H. Zhao, S. Zhang, X. Xu, W. He, L. Zhang, Z. Cheng, *Macromolecules* **2024**, *57*, 756–765, https://doi.org/10.1021/acs.macromol.3c02057.
[47] R. Tamura, T. Kawata, Y. Hattori, N. Kobayashi, M. Kimura, *Macromolecules* **2017**, *50*, 7978–7983, https://doi.org/10.1021/acs.macromol.7b01713.
[48] W. F. Wei, X. Li, K. Jiang, B. Zhang, X. Zhuang, T. Cai, *Angew. Chem. Int. Ed.* **2023**, *62*, e202304608, https://doi.org/10.1002/anie.202304608.
[49] M. Szybowicz, W. Bała, K. Fabisiak, K. Paprocki, M. Drozdowski, *J. Mater. Sci.* **2011**, *46*, 6589–6595, https://doi.org/10.1007/s10853-011-5607-4.
[50] X. Zhang, W. Lin, H. Zhao, R. Wang, *Vib. Spectrosc.* **2018**, *96*, 26–31, https://doi.org/10.1016/j.vibspec.2018.02.009.
[51] E. Ahmetali, A. Galstyan, N. C. Süer, T. Eren, M. K. Şener, *Polym. Chem.* **2023**, *14*, 259–267, https://doi.org/10.1039/D2PY01297A.
[52] H. Cao, M. Gong, M. Wang, Q. Tang, L. Wang, X. Zheng, *RSC Adv.* **2022**, *12*, 5964–5970, https://doi.org/10.1039/D1RA08345G.

[53] D. Li, S. Ge, T. Yuan, J. Gong, B. Huang, W. Tie, W. He, *CrystEngComm* **2018**, *20*, 2749–2758, https://doi.org/10.1039/C8CE00215K.
[54] G. Semushkina, L. Mazalov, S. Lavrukhina, R. Gulyaev, D. Klyamer, T. Basova, *J. Struct. Chem.* **2020**, *61*, 377–387, https://doi.org/10.1134/S0022476620030051.
[55] W. Fan, Z. Duan, W. Liu, R. Mehmood, J. Qu, Y. Cao, X. Guo, J. Zhong, F. Zhang, *Nat. Commun.* **2023**, *14*, 1426, https://doi.org/10.1038/s41467-023-37066-y.
[56] N. Kari, M. Zannotti, R. Giovannetti, D. Řeha, B. Minofar, S. Abliz, A. Yimit, *Nanomaterials* **2022**, *12*, 944, https://doi.org/10.3390/nano12060944.
[57] J. Lee, Y. Kim, S. Park, K. H. Shin, G. Jang, M. J. Hwang, D. Kim, K. A. Min, H. S. Park, B. Han, *Energy & Environ. Mater.* **2023**, *6*, e12468, https://doi.org/10.1002/eem2.12468.
[58] J. McVie, R. S. Sinclair, T. G. Truscott, *J. Chem. Soc., Faraday Trans. 2* **1978**, *74*, 1870, https://doi.org/10.1039/f29787401870.
[59] F. Zhong, J. Zhao, *Dyes Pigm.* **2017**, *136*, 909–918, https://doi.org/10.1016/j.dyepig.2016.09.057.
[60] M. Wang, K. Ishii, *Coord. Chem. Rev.* **2022**, *468*, 214626, https://doi.org/10.1016/j.ccr.2022.214626.
[61] K. Malarz, W. Borzęcka, P. Ziola, A. Domiński, P. Rawicka, K. Bialik-Wąs, P. Kurcok, T. Torres, A. Mrozek-Wilczkiewicz, *Bioorg. Chem.* **2025**, *155*, 108127, https://doi.org/10.1016/j.bioorg.2025.108127.
[62] A. Galstyan, *Chem. Eur. J* **2024**, *30*, e202401305.
[63] J. D. Yi, D. H. Si, R. Xie, Q. Yin, M. D. Zhang, Q. Wu, G. L. Chai, Y. B. Huang, R. Cao, *Angew. Chem.* **2021**, *133*, 17245–17251, https://doi.org/10.1002/ange.202104564.
[64] L.-P. Li, B.-H. Ye, *Inorg. Chem.* **2019**, *58*, 7775–7784, https://doi.org/10.1021/acs.inorgchem.9b00220.
[65] E. L. Clennan, A. Pace, *Tetrahedron* **2005**, *61*, 6665–6691, https://doi.org/10.1016/j.tet.2005.04.017.
[66] A. Golczak, D. Prukała, E. Sikorska, M. Gierszewski, V. Cherkas, D. Kwiatek, A. Kubiak, N. Varma, T. Pędziński, S. Murphree, *Sci. Rep.* **2023**, *13*, 13426, https://doi.org/10.1038/s41598-023-40536-4.
[67] H. Shinohara, O. Tsaryova, G. Schnurpfeil, D. Wöhrle, *J. Photochem. Photobiol.* **2006**, *184*, 50–57, https://doi.org/10.1016/j.jphotochem.2006.03.024.
[68] L. Zhang, X. Shi, Z. Zhang, R. P. Kuchel, R. Namivandi-Zangeneh, N. Corrigan, K. Jung, K. Liang, C. Boyer, *Angew. Chem. Int. Ed.* **2021**, *60*, 5489–5496, https://doi.org/10.1002/anie.202014208.
[69] H. Yang, Z. Lu, X. Fu, Q. Li, L. Xiao, Y. Zhao, L. Hou, *Eur. Polym. J.* **2022**, *173*, 111306, https://doi.org/10.1016/j.eurpolymj.2022.111306.
[70] J. Phommalysack-Lovan, Y. Chu, C. Boyer, J. Xu, *Chem. Commun.* **2018**, *54*, 6591–6606, https://doi.org/10.1039/C8CC02783H.
[71] K. M. Alam, P. Kumar, N. Chaulagain, S. Zeng, A. Goswami, J. Garcia, E. Vahidzadeh, M. L. Bhaiyya, G. M. Bernard, S. Goel, *J. Phys. Chem. C* **2022**, *126*, 15635–15650, https://doi.org/10.1021/acs.jpcc.2c03531.

Manuscript received: October 20, 2025
Revised manuscript received: December 21, 2025
Manuscript accepted: December 31, 2025
Version of record online: ■■, ■■